

THE EFFECTS OF INTERSPACECRAFT COMMUNICATION TIME TAG ERROR ON FORMATION ESTIMATION

Bryan H. KANG Fred Y. HADAEGH Daniel P. SCHARF

*Jet Propulsion Laboratory
California Institute of Technology
4800 Oak Grove Drive, Pasadena, CA 91109*

ABSTRACT - Formation estimation requires inter-spacecraft communication links to exchange sensor measurements and internal data. Mixing asynchronously time-tagged communicated data causes formation estimation errors. Since asynchronous time-tagging can be modeled as a time delay, the impact of these clock-induced estimation errors are characterized as a function of time delay magnitude. This characterization allows the impact of asynchronous time-tagging to be evaluated before costly mitigation strategies (e.g., forced clock synchronization) are undertaken. Several simulation case studies were carried out to demonstrate the effects of time delays. It is shown that in some cases, estimator updates with time-delayed measurements caused more estimation error than update-free estimator propagation.

1 - INTRODUCTION

During a typical spacecraft formation flying mission, streams of time-tagged data are exchanged among formation members. Each formation member can obtain formation state variables, such as relative position and attitude, through either direct measurement and/or through inter-spacecraft communication. For example, the translational state can be propagated by integrating the difference between internal and communicated inertial measurements [Hada 01]. Similarly, relative position and velocity measurements can be communicated between spacecraft for estimator updates. When any two data sets from different spacecraft are mixed and processed according to their attached time-tags, estimation errors will result from differences in their clocks' reference times (i.e., epoch difference).

Two solutions to the asynchronous time-tagging problem are: 1) to force synchronization of every spacecraft's clock, or 2) to bound epoch differences by measuring communication delays and then compensating for the differences using these bounds.¹ Both solutions, however, are costly to implement. Forced clock synchronization is operationally challenging since CPU clocks must be dynamically adjusted; and measuring epoch differences adds complexity to the communication system (e.g., pinging through multiple spacecraft). As both solutions involve considerable effort, it is desirable to first assess the performance loss in a formation estimator if epoch differences are uncompensated.

General formation estimation analysis is challenging because communication and observation links (routes by which information is exchanged and relative measurements are made-See [Kang 01]) can dynamically reconfigure thereby requiring a reconfiguration within the formation estimator as shown in Figure 1.1. Estimator analysis, however, is simplified in the self-centralized estimation architecture introduced in [Kang 01, Hada 01]. In this architecture, state definitions are unaffected by communication routes (i.e., links). The contribution of this paper is to assess the errors induced by asynchronous time-tagging in a self-centralized formation estimator.

¹Reception time-tagging, in which a spacecraft time-tags data as it is received, can bound epoch differences: However, the difference can still drift within the transmission and reception time window.

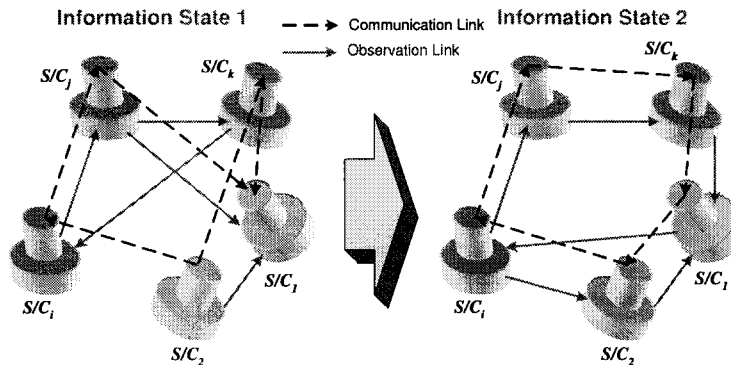


Fig. 1.1: Demonstration of Dynamic Observation Link

2 - MODELING ASYNCHRONOUS TIME-TAGGING

Since a typical spacecraft CPU clock drifts over time due to thermal and calibration errors, epoch differences and the estimation errors they induce will grow. For example, the Deep Space 1 (DS1) spacecraft clock drifts approximately 1 second per week. A CPU's clock drift can be modeled using Allan variance curves [Alla 75, Barn 83] associated with a typical internal quartz oscillator. More simply, clock drift can be modeled as a linear time-invariant system driven by white noises whose intensities are approximated by bounding Allan variance curves (see Figure 2.1). Such a model shows that significant drift occurs on a time scales of hours. Since the estimator error analysis in this paper focuses on estimator convergence which occurs on the time scale of minutes, epoch differences can be modeled as a constant time shift. Subsequently, we refer to epoch differences as *clock delay*, where a “delay” can be positive or negative.

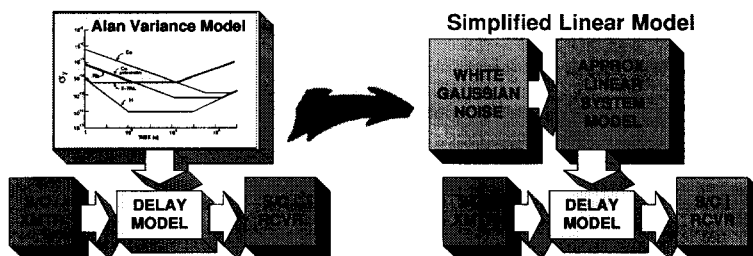


Fig. 2.1: Clock Drift Modeling [Helw 79]

2.1 - Augmentation of Self-Centralized Estimator with Clock Delay Models

Consider an N spacecraft formation with a self-centralized estimator architecture [Kang 01]. Each spacecraft is assumed to have an accelerometer and a limited field-of-view relative position sensor assembly (RPSA), for example, the GPS-like Autonomous Formation Flying (AFF) sensor [Purc 98] or optic-based sensors. For this architecture, the formation state variables are defined as the relative states between the estimator hosting spacecraft and the other spacecraft in a one-to-one manner. More precisely, let the self-centralized estimator be hosted in spacecraft i (S/C_i). The state variables are the relative states (position and velocity) between S/C_i 's and S/C_j 's [respective RPSA's], where $j = 1, \dots, N$, with $j \neq i$. With these architectural assumptions, we now augment the estimator propagation and estimator measurement update steps to include a model of the clock delay.

Augmenting Estimator Propagation Step: Inertial data packets from the other $N - 1$ spacecraft need to be communicated to S/C_i for the propagation of the state variables (i.e., relative velocities and positions). The data sent from S/C_j to S/C_i can be written as:

$$u_{ji} \triangleq M_{jJ} \left[a_{jm}^{JA} + \omega_j^{JB} \times (\omega_j^{JB} \times l_j) + \alpha_j^{JB} \times l_j \right], \quad j = 1, \dots, N \text{ and } j \neq i \quad (2.1)$$

where M_{jJ} is the rotation matrix from S/C_j 's body frame to an inertial frame J , a_{jm}^{JA} is S/C_j 's accelerometer measurement, ω_j^{JB} and α_j^{JB} are the angular rate and acceleration of S/C_j 's body

frame (origin at the center of mass) with respect to frame J , and l_j is the moment arm from S/C_j 's accelerometer to the RPSA.

The signal $u_{ji}(t)$ can be routed to S/C_i through various communication links, but the inertial data is assumed to be time-tagged by S/C_j 's clock. In reference to S/C_i 's time, the signal will appear shifted by a constant value τ_{ji}^o . That is, the signal communicated to S/C_i from S/C_j , $u_{ji}^c(t)$, will be given by $u_{ji}^c(t) = u_{ji}(t + \tau_{ji}^o)$, where τ_{ji}^o is the constant clock delay between S/C_j 's and S/C_i 's clocks. A first order Padé approximation results in the following model for u_{ji}^c :

$$\begin{aligned} \dot{d}_{ji} &= -\frac{2}{\tau_{ji}^o} d_{ji} + u_{ji} \\ u_{ji}^c &= \frac{4}{\tau_{ji}^o} d_{ji} - u_{ji}, \end{aligned} \quad (2.2)$$

where u_{ji}^c is the communicated inertial data in S/C_i time frame and d_{ji} is the delay state.

Augmenting Estimator Measurement Update: Similar to the previous section in which inertial data, u_{ji} , was communicated, communicated RPSA measurements are also impacted by clock delays. RPSA measurements fall into the three categories shown in Table 2.1. In this table, ρ_{ij} is the relative position of S/C_j 's RPSA with respect to S/C_i 's, and n_{ij} is the measurement noise for the RPSA measurement between S/C_i and S/C_j . DIRECT measurements are taken by S/C_i and so there is no clock delay. TYPE I measurements are taken by S/C_j and thus are tagged by the S/C_j 's clock. TYPE II measurements are measurements of S/C_j 's relative position taken by a spacecraft other than the estimator-host, S/C_i . Applying a first order Padé approximation again, the equations for the measurement delay are:

$$\begin{array}{c|c} \text{TYPE I} & \text{TYPE II} \\ \hline \begin{aligned} \dot{y}_{jk} &= -\frac{2}{\tau_{ji}^o} y_{jk} + z_{jk} \\ z_{jk}^c &= \frac{4}{\tau_{ji}^o} y_{jk} - z_{jk} \end{aligned} & \begin{aligned} \dot{y}_{kj} &= -\frac{2}{\tau_{ki}^o} y_{kj} + z_{kj} \\ z_{kj}^c &= \frac{4}{\tau_{ki}^o} y_{kj} - z_{kj} \end{aligned} \end{array} \quad (2.3)$$

where y_{jk} and y_{kj} are the delay states, and τ_{ji}^o and τ_{ki}^o are the constant clock delays of Spacecraft j and k with respect to S/C_i 's clock.

Meas. Class	Meas. Equation	Index	Delay	Description
DIRECT	$z_{ij} = \rho_{ij} + n_{ij}$	for $j = 1 \cdots N, j \neq i$	0	Meas. from S/C_i
TYPE I	$z_{jk} = \rho_{ik} - \rho_{ij} + n_{jk}$	for $k = 1 \cdots N, k \neq j$	τ_{ji}	Meas. from S/C_j
TYPE II	$z_{kj} = \rho_{ij} - \rho_{ik} + n_{kj}$	for $k = 1 \cdots N, k \neq i, j$	τ_{ki}	Any S/C_k to S/C_j

Table 2.1: Measurement Types

3 - COVARIANCE AND ERROR ANALYSIS

To analyze the estimation error induced by clock delays, a self-centered estimator is first designed on a model that has no clock delay elements (e.g. u_{ji} , not u_{ji}^c). Then the model is augmented as described in the previous section. By using Eqns. 2.2 and 2.3 in this augmented model, the model can be reformulated in terms of the estimation error (i.e., the difference between the estimated states and the true states).² The resulting error equation is a function of the estimator input signal (e.g. the spacecraft acceleration profile) and the clock delay magnitude.

After deriving the error equations, three different propagation/update cases are considered. The first case is propagation-only mode. This case occurs during deployment phase before the spacecraft are in each other's fields-of-view or during a blind formation reconfiguration maneuver. The second case adds measurement updates from the estimating spacecraft's own RPSA (i.e., DIRECT measurements in Table 2.1, so there is no clock delay in the measurement update). The third and final case has propagation and measurement updates also, but the

²This approach is similar to a reduced order system analysis, where the covariance equation can be constructed by a higher order plant model and a simplified estimator model.

RPSA measurement is TYPE I (or II), that is, the measurement is communicated from S/C_j (or S/C_k) and so has clock delay.

3.1 - Estimator Design

The spacecraft are assumed to be free-flying, i.e., their relative dynamics are described by a double-integrator model. The truth model, including accelerometer biases, is then

$$\begin{aligned}\dot{b}_i &= \mu_i \\ \dot{b}_j &= \mu_j \\ \dot{V}_{ij} &= -M_{iJ}[b_i + \eta_i] + u_{ii} + M_{jJ}[b_j + \eta_j] - u_{ji} \\ \dot{\rho}_{ij} &= V_{ij},\end{aligned}\tag{3.1}$$

where b_i and b_j are the spacecraft accelerometer biases, μ_i , μ_j , η_i and η_j are the accelerometer bias and bias rate noises, V_{ij} is the relative velocity, u_{ii} is the internal inertial data at S/C_i ((2.1) with j replaced by i) and ρ_{ij} is the relative position. (3.1) depicts an observation link [Kang 01] between S/C_i and S/C_j for any arbitrary j in formation.

For estimator design we use a modified model since only the relative accelerometer bias, $b_i - b_j$, can be measured easily. Rather than estimating this difference directly, however, it is convenient to assume that b_j is a constant, b_j^o , and absorb b_j 's bias noises as well as b_i 's into a new variable b_{ij} with bias noises μ_{ij} and η_{ij} . The modified relative bias b_{ij} and b_j^o contain the same information as $b_i - b_j$. With this modification, the model for estimator design is

$$\begin{bmatrix} \dot{b}_{ij} \\ \dot{V}_{ij} \\ \dot{\rho}_{ij} \end{bmatrix} = \begin{bmatrix} 0 & 0 & 0 \\ -M_{iJ} & 0 & 0 \\ 0 & I & 0 \end{bmatrix} \begin{bmatrix} b_{ij} \\ V_{ij} \\ \rho_{ij} \end{bmatrix} + \begin{bmatrix} 0 \\ M_{jJ}b_j^o + u_{ii} - u_{ji} \\ 0 \end{bmatrix} + \begin{bmatrix} \mu_{ij} \\ -M_{iJ}\eta_{ij} \\ 0 \end{bmatrix}.\tag{3.2}$$

Note that M_{jJ} and b_j^o must also be communicated to S/C_i . When estimator gains H_1 , H_2 and H_3 are designed, the resulting estimator can be written as:

$$\begin{aligned}\hat{b}_{ij} &= H_1(z - \hat{z}) \\ \hat{V}_{ij} &= -M_{iJ}\hat{b}_{ij} - M_{jJ}^c b_j^o + u_{ii} - u_{ji}^c + H_2(z - \hat{z}) \\ \hat{\rho}_{ij} &= \hat{V}_{ij} + H_3(z - \hat{z}),\end{aligned}\tag{3.3}$$

where $(\hat{\cdot})$ signifies an estimate. The measurement z represents any of the measurements listed in Table 2.1. Also, the superscript "c" notation is not applied to b_j^o since it is constant and therefore unaffected by clock delay.

3.2 - Estimation Error Covariance Analysis

Consider the modified communicated inertial data model of

$$\begin{aligned}\dot{d}_{ji} &= -\frac{2}{\tau_{ji}^o}d_{ji} + u_{ji} - M_{jJ}b_j^o \\ u_{ji}^c - M_{jJ}^c b_j^o &= \frac{4}{\tau_{ji}^o}d_{ji} - u_{ji} + M_{jJ}b_j^o\end{aligned}\tag{3.4}$$

and the communicated measurement model of

$$\begin{aligned}\dot{y}_{ji} &= -\frac{2}{\tau_{ji}^o}y_{ji} - \rho_{ij} + n_{ji} \\ z_{ji}^c - \hat{z} &= \frac{4}{\tau_{ji}^o}y_{ji} + \rho_{ij} + \hat{\rho}_{ij} - n_{ji}.\end{aligned}\tag{3.5}$$

The equations (3.1), (3.4) and (3.5) can be combined and rewritten in terms of residual states $b_{ij}^e \triangleq b_{ij} - \hat{b}_{ij}$, $V_{ij}^e \triangleq V_{ij} - \hat{V}_{ij}$, and $\rho_{ij}^e \triangleq \rho_{ij} - \hat{\rho}_{ij}$. The resulting full estimator system dynamics (i.e., estimator plus truth model) can be written as:

$$\begin{aligned}
\begin{bmatrix} \dot{b}_i \\ \dot{b}_j \\ \dot{V}_{ij} \\ \dot{\rho}_{ij} \\ \dot{b}_{ij}^e \\ \dot{V}_{ij}^e \\ \dot{\rho}_{ij}^e \\ \dot{d}_{ji} \\ \dot{y}_{ji} \end{bmatrix} &= \begin{bmatrix} 0 & 0 & 0 & 0 & 0 & 0 & 0 & 0 & 0 \\ 0 & 0 & 0 & 0 & 0 & 0 & 0 & 0 & 0 \\ -M_{iJ} & M_{jJ} & 0 & 0 & 0 & 0 & 0 & 0 & 0 \\ 0 & 0 & I & 0 & 0 & 0 & 0 & 0 & 0 \\ 0 & 0 & 0 & 0 & 0 & 0 & -H_1 & 0 & -H_1 \frac{4}{\tau_{ji}^\circ} \\ 0 & 0 & 0 & 0 & -M_{iJ} & 0 & -H_2 & \frac{4}{\tau_{ji}^\circ} & -H_2 \frac{4}{\tau_{ji}^\circ} \\ 0 & 0 & 0 & 0 & 0 & I & -H_3 & 0 & -H_3 \frac{4}{\tau_{ji}^\circ} \\ 0 & 0 & 0 & 0 & 0 & 0 & 0 & -\frac{2}{\tau_{ji}^\circ} & 0 \\ 0 & 0 & 0 & -I & 0 & 0 & 0 & 0 & -\frac{2}{\tau_{ji}^\circ} \end{bmatrix} \begin{bmatrix} b_i \\ b_j \\ V_{ij} \\ \rho_{ij} \\ b_{ij}^e \\ V_{ij}^e \\ \rho_{ij}^e \\ d_{ji} \\ y_{ji} \end{bmatrix} \\
+ \begin{bmatrix} I & 0 & 0 & 0 & 0 \\ 0 & I & 0 & 0 & 0 \\ 0 & 0 & -M_{iJ} & M_{jJ} & 0 \\ 0 & 0 & 0 & 0 & 0 \\ I & -M_{ji} & 0 & 0 & H_1 \\ 0 & 0 & -M_{iJ} & M_{jJ} & H_2 \\ 0 & 0 & 0 & 0 & H_3 \\ 0 & 0 & 0 & 0 & 0 \\ 0 & 0 & 0 & 0 & I \end{bmatrix} \begin{bmatrix} \mu_i \\ \mu_j \\ \eta_i \\ \eta_j \\ n_{ji} \end{bmatrix} + \begin{bmatrix} 0 \\ 0 \\ u_{ii} - u_{ji} \\ 0 \\ 0 \\ M_{jJ}b_j^\circ - 2u_{ji} \\ 0 \\ u_{ji} - M_{jJ}b_j^\circ \\ 0 \end{bmatrix} &\triangleq FX_e + GW + U.
\end{aligned} \tag{3.6}$$

The estimator system state X_e can be separated into three parts,

$$X_e = X_{e1}|_{X_{e1}(0)=0} + X_{e2}|_{X_{e2}(0)=0} + X_e|_{U=0, W=0}. \tag{3.7}$$

The *stochastic* estimation error contribution due to the sensor driving noises is

$$\dot{X}_{e1} = FX_{e1} + GW \Rightarrow \dot{P}_{xe} = FP_{xe} + P_{xe}F + Q_w, \tag{3.8}$$

where $P_{xe} = E[X_e X_e^T]$, $Q_w = E[WW^T]$, $E[\cdot]$ is the expectation operator and \cdot^T denotes transpose. The *deterministic* estimation error contribution due to the sensor signals is

$$\dot{X}_{e2} = FX_{e2} + U \Rightarrow X_{e2}(t) = \int_0^t e^{F(t-\sigma)} U(\sigma) d\sigma. \tag{3.9}$$

Finally, $X_e|_{U=0, W=0}$ is the zero-input response of the estimation error state.

3.3 - Error Analysis Case 1: Propagation Only

Consider estimator propagation without any measurement updates (i.e., H_1 , H_2 and H_3 are all zero). Recall this situation can happen during a formation initialization or during a reconfiguration maneuver with temporary loss of RPSA lock. Examining only the deterministic portion of the estimation error of (3.6), the residual state (i.e., estimation error) dynamics are

$$\begin{aligned}
\dot{b}_{ij}^e &= 0 \\
\dot{V}_{ij}^e &= -M_{iJ}b_{ij}^e + M_{jJ}(t + \tau_{ji}^\circ)b_j^\circ - [u_{ji}(t) - u_{ji}(t + \tau_{ji}^\circ)] \\
\dot{\rho}_{ij}^e &= V_{ij}^e.
\end{aligned} \tag{3.10}$$

From (3.10) it is seen that the deterministic estimation error is driven by the bias model mismatch $\| -M_{iJ}b_{ij}^e + M_{jJ}(t + \tau_{ji}^\circ)b_j^\circ \|$ and acceleration changes $\Delta u_{ji} \triangleq \| u_{ji}(t) - u_{ji}(t + \tau_{ji}^\circ) \|$ over the clock delay window τ_{ji}° . The second term depends on how fast the acceleration of S/C_j changes over time, thus the error increases as acceleration profiles become steeper.

3.4 - Error Analysis Case 2: Propagation and DIRECT Measurement Update

A DIRECT measurement update (i.e., $z - \hat{z} = \rho_{ij}^e + n_{ij}$) is added to the previous propagation only case of (3.10). Note that the full estimator system equations of (3.6) are for a TYPE I measurement, and so (3.6) is modified to obtain the following Propagation plus DIRECT measurement residual state dynamics:

$$\begin{bmatrix} \dot{b}_{ij}^e \\ \dot{V}_{ij}^e \\ \dot{\rho}_{ij}^e \end{bmatrix} = \begin{bmatrix} 0 & 0 & -H_1 \\ -M_{iJ} & 0 & -H_2 \\ 0 & I & -H_3 \end{bmatrix} \begin{bmatrix} b_{ij}^e \\ V_{ij}^e \\ \rho_{ij}^e \end{bmatrix} + \begin{bmatrix} 0 \\ M_{jJ}b_j^o - \Delta u_{ji} \\ 0 \end{bmatrix} + \begin{bmatrix} \mu_i - M_{iJ}^T M_{jJ} \mu_j - H_1 n_{ij} \\ -M_{iJ} \eta_i + M_{jJ} \eta_j - H_2 n_{ij} \\ -H_3 n_{ij} \end{bmatrix} \quad (3.11)$$

recalling $\Delta u_{ji} \triangleq u_{ji}(t) - u_{ji}(t + \tau_{ji}^o)$. Based on the duality between Linear Quadratic Regulators (LQRs) and Kalman Filters (KFs), (3.11) can be viewed as a disturbance rejection problem with KF feedback. The system will exhibit better disturbance rejection (i.e., lower estimation error) if the estimator design has a larger bandwidth and more gain. Consequently, DIRECT RPSA measurements and applying less weight to the communicated inertial data can reduce the effects of clock delay.

3.5 - Error Analysis Case 3: Propagation and TYPE I Measurement Update

Now consider the case in which S/C_j measures the relative position between itself and S/C_i and communicates this measurement to S/C_i for S/C_i 's estimator update. Since the measurement at S/C_j is $z = -\rho_{ij} + n_{ji}$, the delayed residual can be written as

$$z^c - \hat{z} = \frac{4}{\tau_{ji}^o} y_{ji} - (-\rho_{ij} + n_{ji}) + \hat{\rho}_{ij} = -\rho_{ij}^e + (\rho_{ij}(t) - \rho_{ij}(t + \tau_{ji}^o)) - n_{ji}. \quad (3.12)$$

Applying (3.12) to (3.6) and considering only the deterministic term, results in the following residual state dynamics

$$\begin{bmatrix} \dot{b}_{ij}^e \\ \dot{V}_{ij}^e \\ \dot{\rho}_{ij}^e \end{bmatrix} = \begin{bmatrix} 0 & 0 & H_1 \\ -M_{iJ} & 0 & H_2 \\ 0 & I & H_3 \end{bmatrix} \begin{bmatrix} b_{ij}^e \\ V_{ij}^e \\ \rho_{ij}^e \end{bmatrix} + \begin{bmatrix} -H_1 \Delta \rho_{ij} \\ M_{jJ} b_j^o - \Delta u_{ji} - H_2 \Delta \rho_{ij} \\ -H_3 \Delta \rho_{ij} \end{bmatrix}, \quad (3.13)$$

where $\Delta \rho_{ij} \triangleq \rho_{ij}(t) - \rho_{ij}(t + \tau_{ji}^o)$. The rightmost term of (3.13) shows that nonzero relative velocity (i.e. $\Delta \rho_{ij} \neq 0$) will contribute to the estimation error, and that the error rate is linearly proportional to $\Delta \rho_{ij}$. Since $\Delta \rho_{ij}$ is being multiplied by the estimator gains, estimator designs with higher bandwidths and larger gains will not reduce the clock delay-induced errors.

4 - SIMULATION ANALYSIS

In order to demonstrate the impact of asynchronous time-tagging on formation estimation, a three spacecraft formation example is simulated in MATLAB. The spacecraft are modeled as identical rigid bodies with masses of 308 kg and principal moments of inertia of 79.5, 57.2, and 44.7 kg · m² about the x, y and z body axes, respectively. Each spacecraft is assumed to carry a 6-DOF formation flying sensor suite with an RPSA accuracy of 2 cm. Idealized control (i.e., perfect state feedback) is assumed. This last assumption allows the estimator to operate open-loop and, therefore, the assessment of estimation errors is independent of the particular controller used. That is, controller-estimator interactions are removed from the error assessment.

A triangular formation is initially maintained with 10 m spacecraft separations. Then the formation is expanded to 22-meter separations, as shown in Figure 5.1. Both S/C_2 and S/C_3 communicate inertial data to S/C_1 for its estimator propagation. It is assumed that RPSA measurements are not available between S/C_1 and S/C_3 ; this assumption simulates the propagation-only Case 1. However, both DIRECT and communicated (TYPE I) measurements are available between S/C_1 and S/C_2 to simulate Cases 2 and 3. The estimation errors (residual states) are

obtained by differencing the simulated truth state with the estimates from an estimator designed on a delay-free model. These errors are simulated for various clock delay magnitudes ranging from 0.1 to 1 second.

4.1 - Simulation Results

Case 1 (propagation only) results are shown in Figure 5.2. The upper plot shows the estimator propagation error due to clock delayed accelerometer signals from S/C_3 . During the expansion maneuver, the estimation error can range from 25cm to over 2 meters. The lower plot shows the long-term growth of the estimation error due to uncalibrated accelerometer bias (the short term, deterministic error has been removed for clarity). Figure 5.3 shows the results for Cases 2 and 3. In the upper plot DIRECT RPSA measurement updates reduce the clock delay-induced errors resulting from communicated inertial data, and they calibrate the relative accelerometer bias. TYPE I RPSA measurements, however, are also clock delayed (lower plot of Figure 5.3), and so measurement updates no longer improve estimates during a maneuver. The estimation error can be *worse* than in propagation-only estimation.

5 - CONCLUSIONS

Asynchronous time-tagging of communicated data in a formation will induce estimation errors. These errors were first analyzed and then assessed through simulation as a function of the magnitude of the epoch difference between spacecraft clocks. When no measurement updates are done by the estimator (i.e., propagation-only mode), the clock delay-induced estimation error depends on the steepness of the acceleration profiles of the spacecraft. Relative position measurements made by the estimator-hosting spacecraft can reduce the size of this acceleration profile-error. It was shown that the larger the estimator feedback gain and bandwidth, the more clock delay-induced errors are attenuated. However, when communicated relative position measurements are used for estimator measurement updates, the clock delay-induced estimation error can become worse. In the simulated examples, the estimation error doubled from the propagation-only case. Since the estimator gains multiply the communicated relative position measurements, increasing the estimator's gain does not attenuate the clock delay effects, rather, it increases the error.

ACKNOWLEDGEMENTS

This research was performed at the Jet Propulsion Laboratory, California Institute of Technology, under contract with the National Aeronautics and Space Administration.

REFERENCES:

- [Alla 75] Allan D.W., "The Measurement of Frequency and Frequency Stability of Precision Oscillators," *Proceedings of the 6th PTTI Planning Meeting*, p109, 1975
- [Barn 83] Barnes J.A., "The Measurement of Linear Frequency Drift in Oscillators," *Proceedings of the 15th Annual PTTI Meeting*, 1983
- [Hada 01] Hadaegh F. Y., Kang B. H., Scharf D. P., "Rule-Based Formation Estimation for Distributed Spacecraft," *Tenth IEEE International Conference on Fuzzy Systems*, 2001.
- [Helw 79] Hellwig H., "Microwave time and frequency standards," *Radio Science*, 14(4), 561-572, 1979
- [Kang 01] Kang B. H., Hadaegh F. Y., Scharf D. P., Ke N.P., "Decentralized and Self-Centered Estimation Architecture for Formation Flying of Spacecraft," *16th International Symposium on Space Flight Dynamics*, Pasadena, California 2001
- [Purc 98] Purcell, G.; Kuang, D.; Lichten, S.; Wu, S. and Young, L., "Autonomous Formation Flyer (AFF) Sensor Technology Development," *21st AAS Guidance and Control Conference*, 1998.

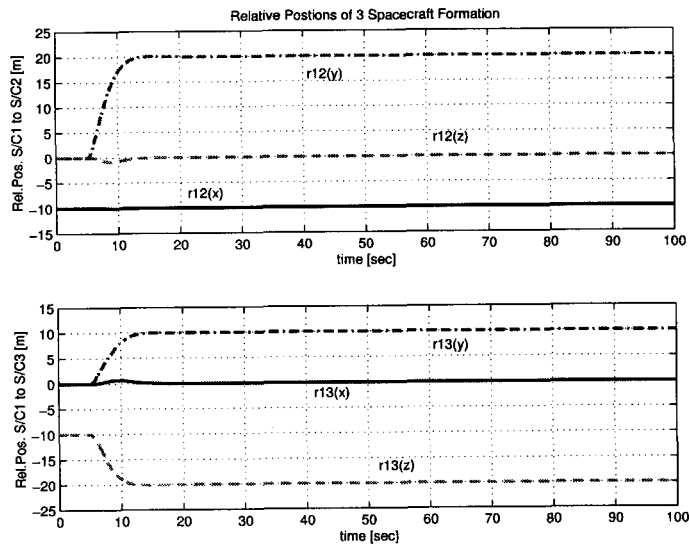


Fig. 5.1: Spacecraft Relative Position, Responding to a Formation Expansion Command

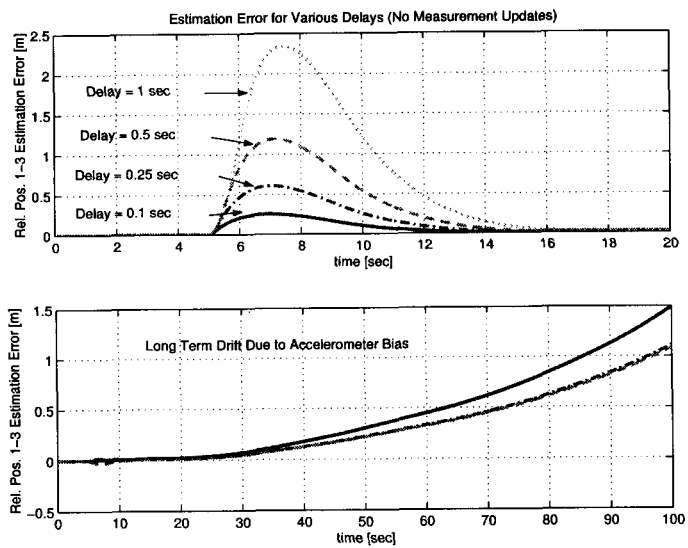


Fig. 5.2: CASE 1: Free Propagation without Measurement Updates

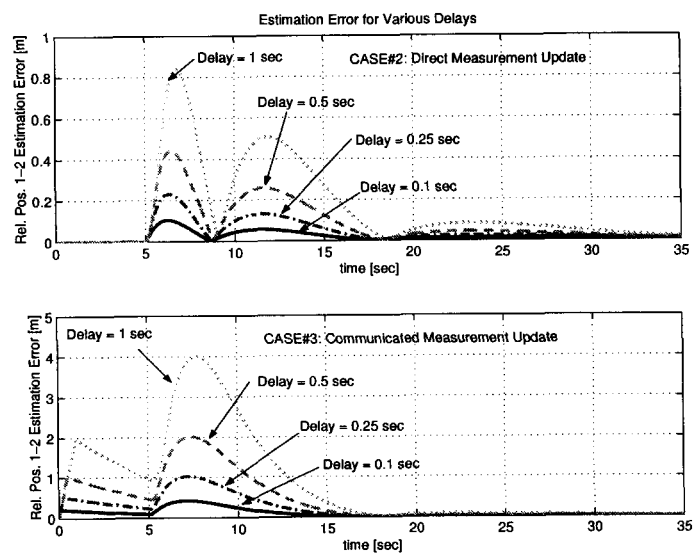


Fig. 5.3: CASE 2 & 3: Direct and Communicated Measurement Updates